Preprint Title	First series of *N*-alkylamino peptoid homooligomers: Solution phase synthesis and conformational investigation
Authors	Maxime PYPEC, Laurent JOUFFRET, Claude TAILLEFUMIER and Olivier ROY
Publication Date	10 Mai 2022
Article Type	Full Research Paper
Supporting Information File 1	ESI_Taillefumier.pdf; 5.6 MB
Supporting Information File 2	MP420.cif; 3.8 MB
Supporting Information File 3	checkcif_MP420.pdf; 73.5 KB
ORCID® iDs	Maxime PYPEC - https://orcid.org/0000-0003-3720-7438; Laurent JOUFFRET - https://orcid.org/0000-0003-0196-7128; Claude TAILLEFUMIER - https://orcid.org/0000-0003-3126-495X; Olivier ROY - https://orcid.org/0000-0002-7238-8708

First series of *N*-alkylamino peptoid homooligomers: Solution phase synthesis and conformational investigation

Maxime Pypec, Laurent Jouffret, Claude Taillefumier*‡, and Olivier Roy‡

Université Clermont Auvergne, Clermont Auvergne INP, CNRS, ICCF, F-63000 Clermont–Ferrand, France.

Email: Claude Taillefumier – claude.taillefumier@uca.fr

* Corresponding author

‡ Equal contributors

Abstract

The synthesis and conformational analysis of the first series of peptoid oligomers composed of consecutive *N*-alkylamino glycine units is investigated. We demonstrate that *N*-methylamino glycine homooligomers can be readily synthesised in solution using N-Boc-N-methylhydrazine as a peptoid submonomer and stepwise or segment coupling methodologies. Their structures were analyzed in solution by 1-D and 2-D NMR, in the solid state by X-ray crystallography (dimer **2**) and implicit solvent QM geometry optimisations. *N*-methylamino peptoids were found to preferentially adopt *trans* amide bonds with the side chain N-H bonds oriented approximately perpendicular to the amide plane. This orientation is conducive to local backbone stabilization through intra-residue hydrogen bonds but also to intermolecular associations. The high

capacity of *N*-methylamino peptoids to establish intermolecular hydrogen bonds was notably deduced from pronounced concentration dependent N-H chemical shift variation in ^{1}H-NMR, the antiparallel arrangement of mirror images molecules held together via two hydrogen bonds in the crystal lattice of dimer **2**, and self-assembling properties of dimer **2** visualized by transmission electron microscopy.

Keywords

peptoid; *cis*/*trans* isomerism; *trans*-inducing side chain; structure

Introduction

The term “peptoids” refers to the family of artificial oligo-(poly)mers consisting of *N*-substituted glycines [1,2]. They retain the same backbone as peptides - except that the side chains are located on the nitrogen atoms of the amide bonds - and thus represent an important class of peptide biomimetics[3–5], generally with improved cell permeability[6] and proteolytic resistance [7,8]. Beyond their resemblance to peptides, the obvious interest in this family of peptidomimetics arises from their ease of synthesis by the modular submonomer protocol [9] which enable the incorporation of numerous primary amine synthons in a sequence-controlled manner[10], and application of solid-supported combinatorial approaches [11–13]. The most relevant comparison of peptoids with peptides is in fact with polyprolines due to the presence of backbone tertiary amide linkages, much more prone to *cis*/*trans* equilibria than secondary amides. Indeed, in proteins, *cis*- amide bonds are most often observed for Xaa–Pro amide bonds and polyproline chains can adopt either the all-*trans* type II (PPII) or the all-*cis* type I (PPI) helical conformations, the latter being only observed in alcohol-type solvents [14]. In contrast to the prolyl-amide bond in acyclic peptides (~5% of *cis*-Pro)

[15], the *cis* conformation of peptoid amide bonds is generally much more populated, leading to substantial conformational heterogeneity [16]. Thus, adoption of well-defined secondary structures requires fine control of backbone amide isomerism. Considerable efforts have been made to regulate the conformation of peptoids through steric and electronic interactions involving peptoid amides and nearby side chains [17,18]. For example, *N*-substituted monomers bearing benzylic-type *N*α-chiral groups including the phenylethyl [19–21], naphthylethyl [17,22–24], and triazolium groups [25–27], alkyl ammonium [28], *tert*-butyl/α,α-gem-dimethyl [29], or fluorinated groups [30] will preferentially form *cis*-amides (Fig. 1A). Peptoid helicity modulation has also been investigated through specific placement of chiral and achiral monomers.[31,32] Comparatively, fewer *N*-functional monomers capable of promoting *trans* peptoid amides were designed. Among these are the *N*-aryl [33–35], *N*-hydroxy [36], *N*-alcoxy [37], and *N*-(acylhydrazide)glycines (Fig. 1A) [38,39]. Recently, while our work was in progress, *N*-imino and *N*-alkylamino glycines have also been proposed to build up peptoids with *trans* amide bonds [40]. In this seminal publication, hydrazones were utilized as submonomers in the displacement step of resin-bound bromoacetylated peptoids and cleavage from the resin with TFA containing 5% of triethylsilane resulted in a concomitant reduction of the imine functions in *N*-alkylamino groups. In this work, however, the *N*-alkylamino-containing glycine units were not introduced consecutively but every two or three residues. We describe here the synthesis and study of the first representatives of peptoids containing exclusively *N*-alkylamino-substituted amides. As the first representatives of this family we chose to synthesise peptoid oligomers containing *N*-substituted methylamino amides, considering that the methods developed could be used for the synthesis of other members of this family (Fig. 1B).

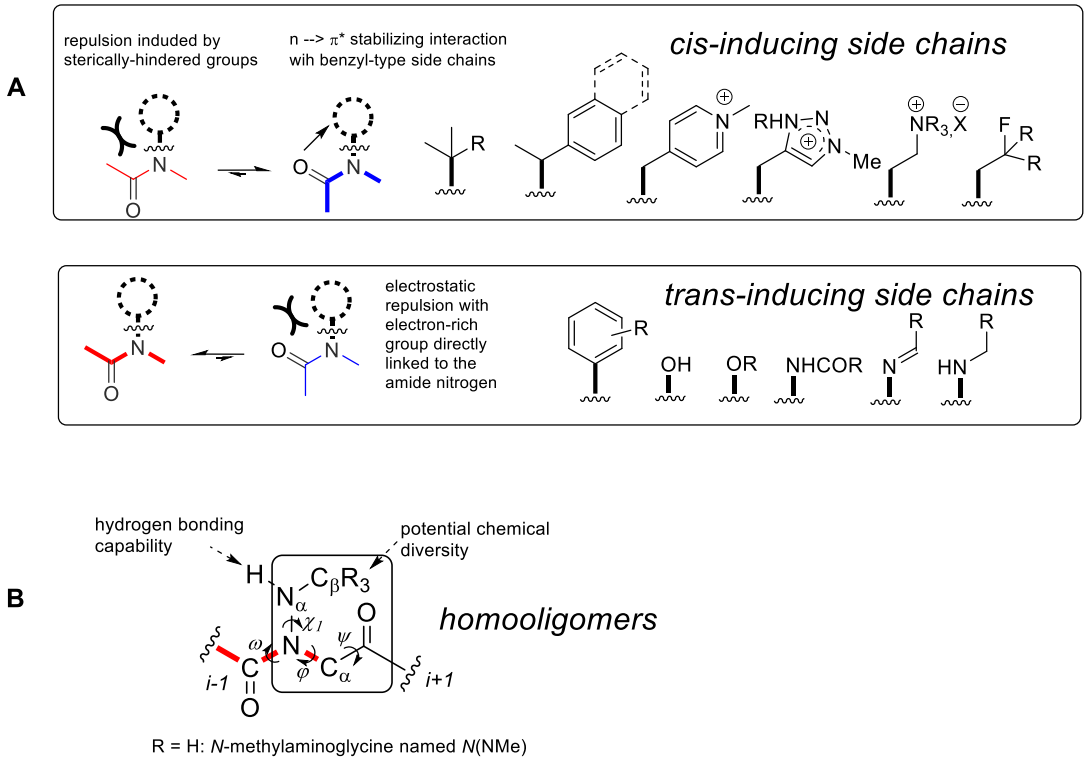

Figure 1: (A) Summary of the main side chains exerting significant steric and/or electronic effects and influencing the amide conformation of peptoids. (B) Atom labels in *N*-methylaminoglycine monomers

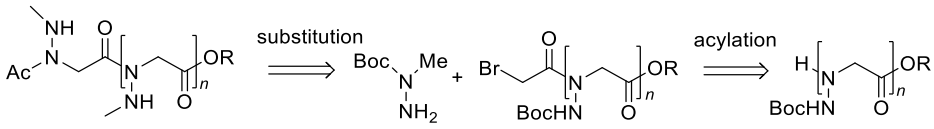

Figure 2: Solution-phase synthesis of *N*-(methylamino)glycine oligomers using N-Boc-N-methylhydrazine as a submonomer

Results and Discussion

Synthesis

A solution-phase approach using commercially available *N*-Boc-*N*-methyl hydrazine as a submonomer was adopted in this work (Fig. 2). Benzyl bromoacetate, rather than *tert*butyl bromoacetate, successfully used in the past for the synthesis of peptoids in

solution [22], was chosen as the starting substrate to ensure orthogonality of the *C*-terminal protecting group with respect to the Boc side chain protections. For the submonomer solution-phase synthesis of monomer **1** and oligomers **2-5**, modifications from the standard synthesis conditions were required, notably for the substitution reaction. Thus, the first substitution reaction between benzyl bromoacetate and *N*-Boc-*N*-methyl hydrazine (3.0 eq.) was conducted in water at a concentration of 2.5 M at room temperature (rt) for overnight to afford monomer **1a** in 88% yield after SiO_2-chromatography [41]. Standard substitution conditions in EtOAc or THF as solvent in the presence of triethylamine did not allow full conversion of the starting bromoacetate at rt or on heating to 50 °C. The further substitution reactions, during peptoid elongation, were carried out in a 1:1 MeOH/H_2O mixture (1.25 M) at 60 °C, using three equivalents of the Boc-protected hydrazine reagent. These distinct substitution conditions, together with standard acylation conditions in solution (Scheme 1) allowed us to reach the pentamer length with good yields for each substitution-acylation submonomer cycle (from 56 to 76% yield, ESI, Scheme S1). All compounds were acetylated at the *N*-terminus followed by removal of the Boc protecting groups to obtain peptoids **1**-**5** with high purity at the scale of several hundred milligrams (Table 1). Synthesis details are provided in the ESI, along with analysis data. The main limitation of this synthetic route is the somewhat delicate purification of the products after the substitution step, due to the close polarities of the products and starting hydrazine reagent. So we turned our attention to a fragment-based coupling approach for synthesising the hexamer peptoid **6**.

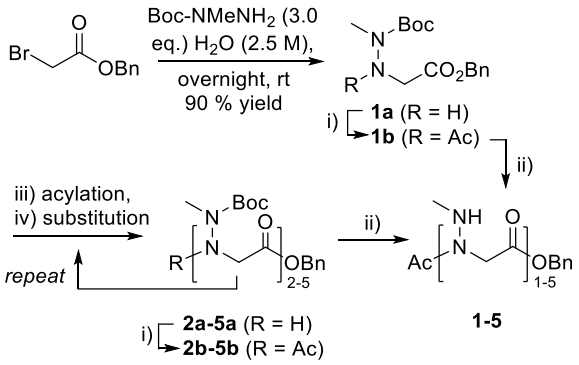

Scheme 1. Submonomer synthesis used for the construction of peptoids **1-5** containing *N*-methylamino side chains. Conditions: i) Ac_2O (8.0 eq.), Et_3N (4.0 eq.), EtOAc (0.2 M), rt, 48h; ii) TFA/CH_2Cl_2 (1:1), 0 °C to rt, 30 min; iii) $BrCH_2COBr$ (1,5 eq.), Et_3N (2.0 eq.), THF (0.2 M), -10°C, from 30 min to 2 h; iv) *N*-Boc-*N*-methyl hydrazine (3.0 eq.), H_2O/MeOH 1:1 (1.25 M), 60°C, overnight.

Thus, several coupling methods were evaluated, initially starting from the hydrazine and acid monomers **1a** and **1c**, respectively (Scheme 2). The *N*-Fmoc protected acid partner **1c** was readily prepared from **1a** under standard conditions. After a few unsuccessful attempts of coupling using the azabenzotriazole-based coupling reagent HATU [42] or via the formation of an acid chloride with thionyl chloride, we turned to the mixed anhydride activating method using isobutyl chloroformate (IBCF) in the presence of *N*-methylmorpholine (NMM) at 0 °C in DMF for 10 min, followed by the addition of hydrazine **1a** [43,44]. The best results were obtained with two equivalents of preformed mixed anhydride, pure dimer **2d** being isolated in 78% yield after chromatography. The use of stoichiometric amounts of both partners led to incomplete conversion, with about 1/3 of the starting hydrazine being recovered after two days of reaction. We then tested 2-ethoxy-1-ethoxycarbonyl-1,2-dihydroquinoline (EEDQ), in dioxane, a method for *in situ* generation of a mixed anhydride [45]. This method gave the highest coupling yield to dimer **2d**, but again with the condition of using an excess

of the acid partner, as some of it was consumed to give the by-product ethyl ester **1e**. Dimer **2d** was obtained for example in 95% yield from 1.5 equivalents of acid and carrying out the reaction at 60 °C. The formation of by-product **1e** was also observed at room temperature and attempts to trap the ethanol released in the reaction by molecular sieve did not give any improvement.

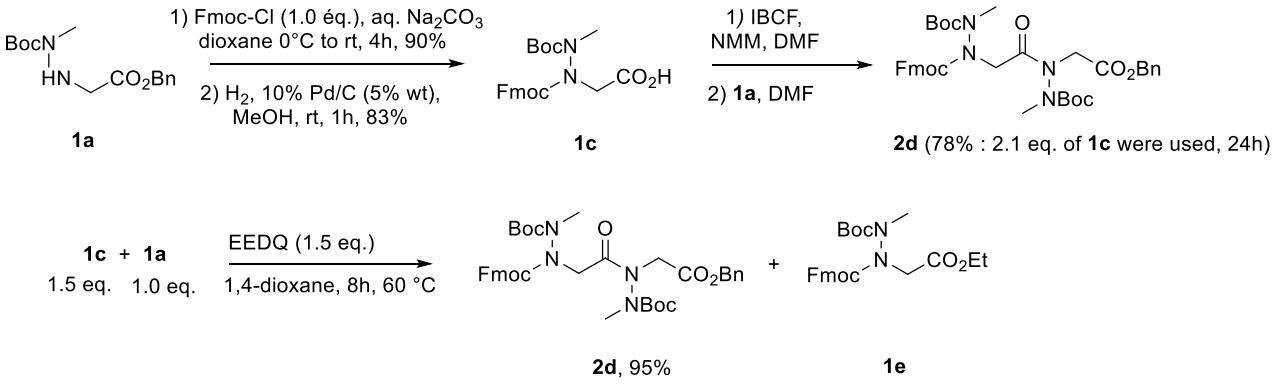

Scheme 2. Evaluation of the efficiency of mixed anhydride methods by coupling of **1a** and **1c**.

Finally, we tested *N*-methyl-2-chloropyridinium iodide (Mukaiyama reagent)[46] by applying the method to a (3+3) segment coupling of the *N*-acetylated trimer **3-OH** onto trimer hydrazine **3a**, in equimolar proportions, resulting directly in hexamer **6** after removal of the Boc groups (Scheme 3). In this way, the desired peptoid **6** was isolated in a satisfactory yield of 47% (2 steps) after coupling and TFA-mediated Boc removal.

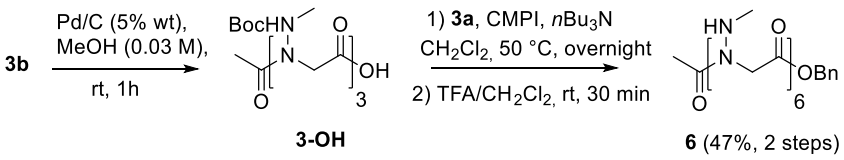

Scheme 3. (3+3) segment coupling of trimers **3-OH** onto trimer hydrazine **3a**.

Table 1. Structures, purity, retention time, and calculated and observed masses for peptoids **1**-**6**

peptoid	Sequence	% purity[a]	retention time	calculated mass	observed mass
1	Ac-*N*NMe-OBn	100	8.18	236.1161	237.1234 $[M+H]^+$
2	Ac-(*N*NMe)$_2$-OBn	98	7.71	322.1641	323.1714 $[M+H]^+$
3	Ac-(*N*NMe)$_3$-OBn	97	7.57	408.2121	409.2194 $[M+H]^+$
4	Ac-(*N*NMe)$_4$-OBn	93	7.55	494.2601	495.2674 $[M+H]^+$
5	Ac-(*N*NMe)$_5$-OBn	92	7.55	580.3081	581.3152 $[M+H]^+$
6	Ac-(*N*NMe)$_6$-OBn	98	7.85	666.3562	667.3625 $[M+H]^+$

[a] Determined from the HPLC UV trace at 214 nm (conditions in ESI)

Structural characterization of *N*-methylamino peptoid oligomers

X-ray diffraction analysis of peptoid dimer 2.

Peptoid dimer **2** was crystallized by slow evaporation from chloroform, and its high resolution structure was determined by X-ray crystallography. The crystal structure of dimer **2** confirms the *trans* geometry of the two amide bonds (Fig. 3A). The unit cell contains eight molecules, including two groups of four identical molecules (Fig. 3B), the conformation of the first group (conformation A, Table 2) being the mirror image of that observed for the second group of molecules (conformation B). In the crystal lattice, each molecule establishes four intermolecular CO---HN hydrogen bonds. Only the inter-residue carbonyl (oxygen atom labeled O2, Fig. 3C) participate in this network, making two hydrogen bonds with two different molecules and different NH groups (labelled H10 and H11, Fig. 3C). The φ and ψ dihedral angle values are comparable to those measured by X-ray diffraction of monomers bearing benzylamino side chains,[40] and of an *N*-aryl[33] and *N*-hydroxy peptoid dimers [36]. The latter dimer with φ angles of opposite sign was shown to form a unique sheet-like secondary structure, whereas molecular modeling showed that *N*-aryl peptoid oligomers composed of monomers in the same conformation (as observed in the crystal of dimer **2**) might adopt right or left-handed helical conformations that resemble the polyproline

type II helix. The $\chi 1$ dihedral angles, -111.6 and -116.1 for residues 1 and 2, respectively (conformation A), are identical to one another in sign, a sign that corresponds to that of the φ dihedral angles. This results in an almost perpendicular orientation of the N-H bond with respect to the amide plane and a proper orientation of the NH and CO groups of the same residue for intramolecular hydrogen bonding, although the N...O distances of 3.13 and 3.30 Å are slightly above the accepted thresholds.

Table 2. Dihedral angles observed in dimer **2** crystal structure

	residue	ω (°)	φ (°)	ψ (°)	$\chi 1$ (°)	d ^{i}Nα---OC^{i} (Å)
conformation A	1	–176.5	–87.7	166.7	–111.6	3.30
	2	–173.7	–103.3	167.1	–116.1	3.13
conformation B	1	176.5	87.7	–166.7	111.6	3.30
	2	173.7	103.3	–167.1	116.1	3.13

Dihedral angles definition: ω [Cα(i-1); C(i-1); N; Cα], φ [C(i-1); N; Cα; C], ψ [N; Cα; C; N(i+1)], χ_1 [C(i-1); N; N_α; C_β].

A

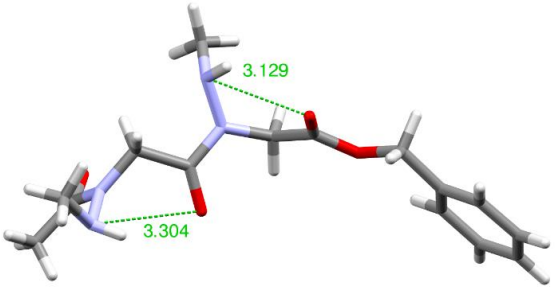

B

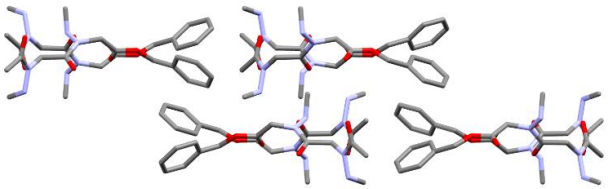

C

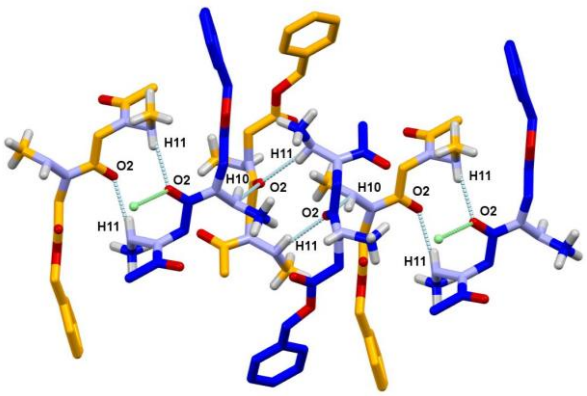

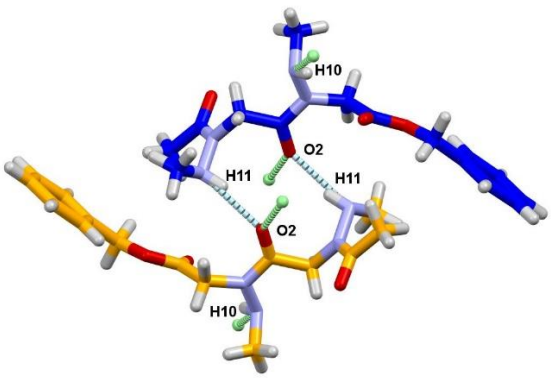

Figure 3. X-ray crystal structure of peptoid dimer **2**: (A) single molecule; (B) unit cell, view along b axis (hydrogen atoms removed for clarity); (C) overview of the hydrogen bonding network (conformation A depicted in blue, conformation B in orange), hydrogen bonds (light blue dashed lines), hanging hydrogen bonds (light green dashed lines)

Conformational analysis and self-assembling properties

1H NMR analysis of monomer **1** in various solvents including $CDCl_3$, CD_3CN, C_6D_6, CD_3OD, D_2O, and DMSO-d_6 showed two sets of resonances in proportions varying from 75:25 to 90:10 (Table 3). These two sets of signals were characterized as the backbone *cis* and trans-amide rotamers using NOESY experiments (Fig. 4 and ESI) Specifically, in DMSO-d6, the predominant rotamer of monomer **1** is characterized by a NOE cross-peak between the acetyl methyl group and side chain methyl group, indicative of a *trans*-amide bond geometry. A NOE cross-peak between the backbone methylene group and side chain methyl group is also observed in this *trans*-rotamer. For the second set of resonances, the presence of a NOE cross-peak between the backbone methylene group and acetyl methyl group confirmed the presence of a *cis*-amide bond. Similarly, dimer **2** and trimer **3** showed similar correlation patterns to those observed in the monomer involving two and three *trans*-amide bonds, respectively for the predominant rotamers (Fig. 4 and ESI).

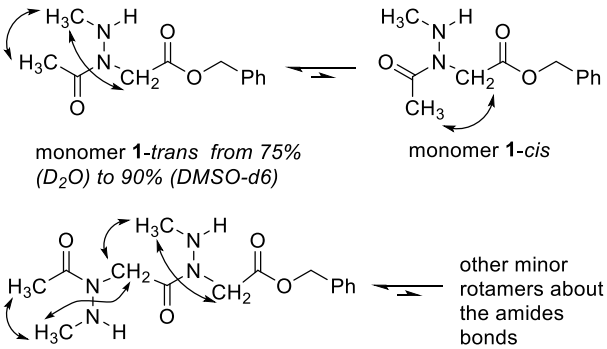

dimer **2**-*trans-trans from 61% (D_2O) to 79% (DMSO-d6)*

Figure 4. NOE effect interaction observed in the 2D-NOESY spectra of monomer **1** and dimer **2** in DMSO-d_6.

We could also show that the two amides of dimer **2** have approximately the same *cis*/*trans* ratio, at least in $CDCl_3$ and CD_3OD. This suggests that the same may be true for longer oligomers. As the oligomer elongates, shoulders that may represent different rotamers in small proportions appear in the NMR spectra, but one isomer remains present predominantly. More specifically, in the case of trimer **3**, tetramer **4**, pentamer **5** and hexamer **6**, we were able, for example, to establish that the majority rotamer is present at 70%, 84%, 80% and 86%, respectively in DMSO-d_6, based on the integration of the backbone methylene signals. Overall, DMSO seems to be the most structuring solvent for these oligomers, followed very closely by methanol and acetonitrile.

Table 3. Average *trans* rotamer proportions (% *trans*) and $K_{cis/trans}$ values in peptoids **1** and **2**, calculated from the integration of ^{1}H NMR spectra in various solvents (8 mM).

	$CDCl_3$		C_6D_6		$(CD_3)_2SO$		CD_3CN		CD_3OD		D_2O	
	% trans	$K_{cis/trans}$	% trans	$K_{cis/trans}$	% trans	$K_{cis/trans}$	% trans	$K_{cis/trans}$	% trans	$K_{cis/trans}$	% trans	$K_{cis/trans}$
1	82	0.22[b]	84	0.18[b]	90	0.11[b]	85	0.17[c]	89	0.13[b]	75	0.34[a]
2	77	0.31[b]	[d]	[d]	79	0.26[b]	78	0.29[b]	75	0.33[b]	61	0.63[c]

[a] calculated by averaging the integrations of 4 signals from the NMR spectrum. [b]calculated by averaging the integrations of 3 signals from the NMR spectrum. [c]calculated by averaging the integrations of 2 signals from the NMR spectrum. [d]not measurable.

Having confirmed that the *N*-methylamino amide bonds of the synthesised oligomers are mainly in the *trans* conformation, it remained to be seen whether the NH of the side chains participate in hydrogen bonding either intra- or intermolecularly.

The ^{1}H-NMR resonances of the N-H groups of peptoids **1-5** displayed broad signals at room temperature in $CDCl_3$. This is likely due to proton exchange between various NH groups in low polar solvents or to exchanges between the NH protons and protons of residual H_2O. In weakly polar aprotic solvents such as $CDCl_3$, resonance broadening may also be due to intermolecular association. The chemical shift of donor protons (D-

H) involved in intermolecular hydrogen bonds is generally very sensitive to concentration change. A variable concentration ^{1}H-NMR study of monomer **A** and trimer **3** was carried out in $CDCl_3$. The piperidinyl amide-capped monomer **A** (Fig. 5, see ESI for synthesis), was preferred to monomer **1** to allow an unbiased comparison with a previous study from the Proulx group (monomer **B**, Fig. 5).[40] A large variation in the chemical shift of NH was observed over a concentration range of 2-50 mM for monomer **A** in $CDCl_3$ ($\Delta\delta$ = 3.09 ppm, ESI, Fig. S1), suggesting intermolecular hydrogen bonding, in sharp contrast to the $\Delta\delta$ = 0.01 ppm measured for the piperidinyl amide-capped *N*-benzylamino glycine monomer **B**, which is further characterized by a narrow NH signal in $CDCl_3$ or DMSO-d_6 (Fig. 5). The same behaviour was observed in the case of trimer **3** ($\Delta\delta$ = 2.61 ppm), again suggesting intermolecular hydrogen bonding. The minimal steric hindrance of the side chain *N*-methyl group thus seems favorable to intermolecular associations, as observed in the case of *N*-hydroxypeptoids [36]. Another notable difference between monomers **A** and **B** is the large difference in chemical shift of the NH group at a given concentration (3.25 ppm for **A** and 4.92 ppm for **B** at 10 mM in $CDCl_3$). The significant deshielding of the NH chemical shift in **B**, as compared to **A**, is consistent with intramolecular hydrogen bond interaction, which is accompanied by a reduction of the exchange rate of the NH proton. In DMSO, we observe reduced NH linewidths, consistent with the fact that this solvent has strong hydrogen bonding and solvation abilities which reduce significantly proton exchange. Overall, the NMR study suggest that the *N*-methylamino glycine monomer and oligomers have a strong propensity to form intermolecular hydrogen bonds, an interesting and sought-after property for self-assembling and interaction with biological targets.

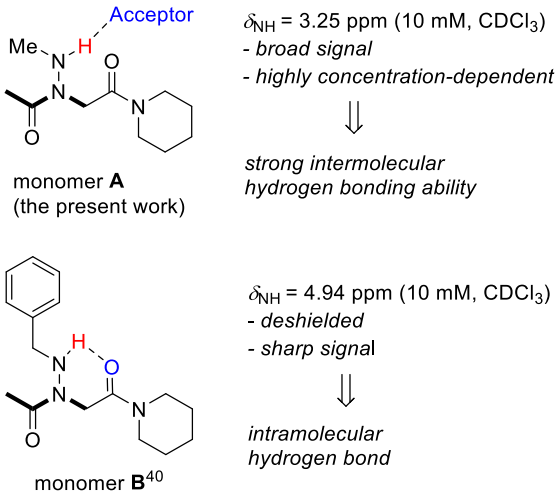

Figure 5. comparison of monomers **A** and **B** with respect to their ability to form intramolecular and intermolecular hydrogen bonds.

Neat peptoids **1**-**6** were also characterised by Fourier-transform infrared spectroscopy. The spectra show two distinct N-H stretching bands in the 3500-3200 cm^{-1} region whose relative intensity varies with chain elongation. A first band, the more intense of the two, is observed at about 3300 cm^{-1}. A higher energy band of much lower intensity at about 3450-3500 cm-1 is also observed, especially from the trimer stage. We can assume that the lower energy bands (3300 cm^{-1}) are due to hydrogen-bonded N-H while the higher energy bands could be attributed to non-hydrogen bonded NH. This observation may indicate that not all NHs can form hydrogen bonds within an assembly, and that this is dependent on the size of the oligomers. Also, the region of the spectra corresponding to the C=O stretching (1800-1600 cm^{-1}) show a band at 1743 cm^{-1} corresponding to C=O stretching of the ester and a band at 1648 cm^{-1} which increases with the oligomer length, corresponding to the amide I C=O stretching of the N-methylamino amides functions.

The self-assembling properties of this family of oligomers are illustrated by the Transmission Electronic Microscopy (TEM) images (TEM) collected from dimer **2** (1

wt% in water) showing ordered self-assembled multilayered structures (Fig. 6 and Fig. S5) At this stage, we cannot yet propose a mode of interaction that explains the formation of these assemblies. Furthermore, it is not possible to say whether the structure of molecule **2** in the assemblies is the same as in the crystal, i.e. with the two monomers in the same conformation. Indeed, it is known, for example, that an N-hydroxy peptoid dimer that self-assembles into sheet-like structure has two units in mirror-image conformations. In any case it is interesting to note that it is one of the few examples of a peptoid structure with that of the N-hydroxypeptoids to show self-assembly based on hydrogen bonds, and not on aromatic π–π stacking [47] or oppositely charged pendant groups [48].

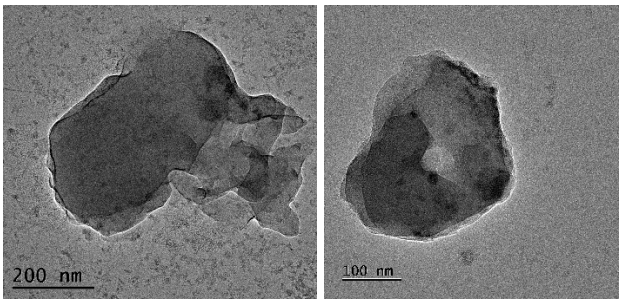

Figure 6. TEM images of the assemblies of dimer **2** at 10 mg mL^{-1} in water.

Computational studies

For the theoretical calculations, acetyl *N*-methylamino dimethylamide model peptoids (Ac-*N*(NMe)*n*-NMe_2) were used instead of the corresponding synthesized benzyl esters. The model structures were generated using the coordinates extracted from the single crystal X-ray diffraction data of dimer **2**. Geometry optimizations were carried out with the B3LYP/6-31G(d,p) basis set as implemented in Gaussian 16, using tight convergence criteria (opt=tight) in chloroform (scrf=(solvent=chloroform)).

We first examined the preferred amide-bond geometry by a relaxed potential energy surface (PES) scan about the ω dihedral angle with a scan interval of 10° in 35 steps from -180° to 180°.The global minimum energy was observed at -174° and +176°, with

a substantial energetic preference for the *trans*-amide bond of 6.5 kcal/mol, supporting the *trans* geometry determined from NMR and X-ray diffraction experimental data (Fig. S3). To understand how the methylamino-substituent will be oriented on oligo-*N*NMe peptoids, we have also performed a $\chi 1$ angle relaxed PES scan of acetyl-*N*-methylamino glycine-dimethylamide (Fig. S4). The lowest energy was found for $\chi 1$ = 124°, an angle value slightly higher than those found in the crystallographic structure of compound **2** (111 and 116° for conformation B, Table 2). This difference may be a result of the 6-membered intramolecular hydrogen bond formed in the monomer model (d N...O = 2.88 Å, $\angle^{i}$N-H···O = 125°, Table S1). Two hydrogen bonds were also present upon geometry optimization of the dimer model Ac-*N*-$(NMe)_2$-NMe_2 (Table S2).

In the crystallographic structure of dimer **2**, the two constitutive monomers of a molecule are in the same conformation with either two positive values of the φ angle (conformation B) or two negative values for the mirror image conformation A. These two local conformations could exist at each monomer position, leading to a potential mixture of secondary structures. We therefore calculated the relative energy difference between the structure of a dimer consisting of two monomers in the same conformation (pp) with that of a dimer structure with monomers in two different mirror image conformations (pm) (Fig. 5A,B). We found that the repeating (pp) conformation is only favored by 0.65 kcal.mol^{-1} over the (pm) alternated conformation, suggesting that these two conformations could coexist in solution. Furthermore, the (pm) dimeric model adopt a structure analogous to the solid-state structure of an *N*-hydroxypeptoid dimer, with very similar dihedral angles and φ angles opposite to one another in sign.[36] Calculation was also carried out at the hexamer length considering only the repeating $(p)_6$ and alternating $(pm)_3$ regular conformations (Table S3). It resulted that the

repeating conformation $(p)_6$ is most stable by 2.9 Kcal.mol^{-1} and form an extended right-handed helical conformation with backbone torsion angle (φ, ψ) values in vicinity of (100°, -173°), approximately 3 residues per turn and a helical pitch of 10 Å (Fig 5C). The structure resembles the type II polyproline helix, with a slightly larger pitch.

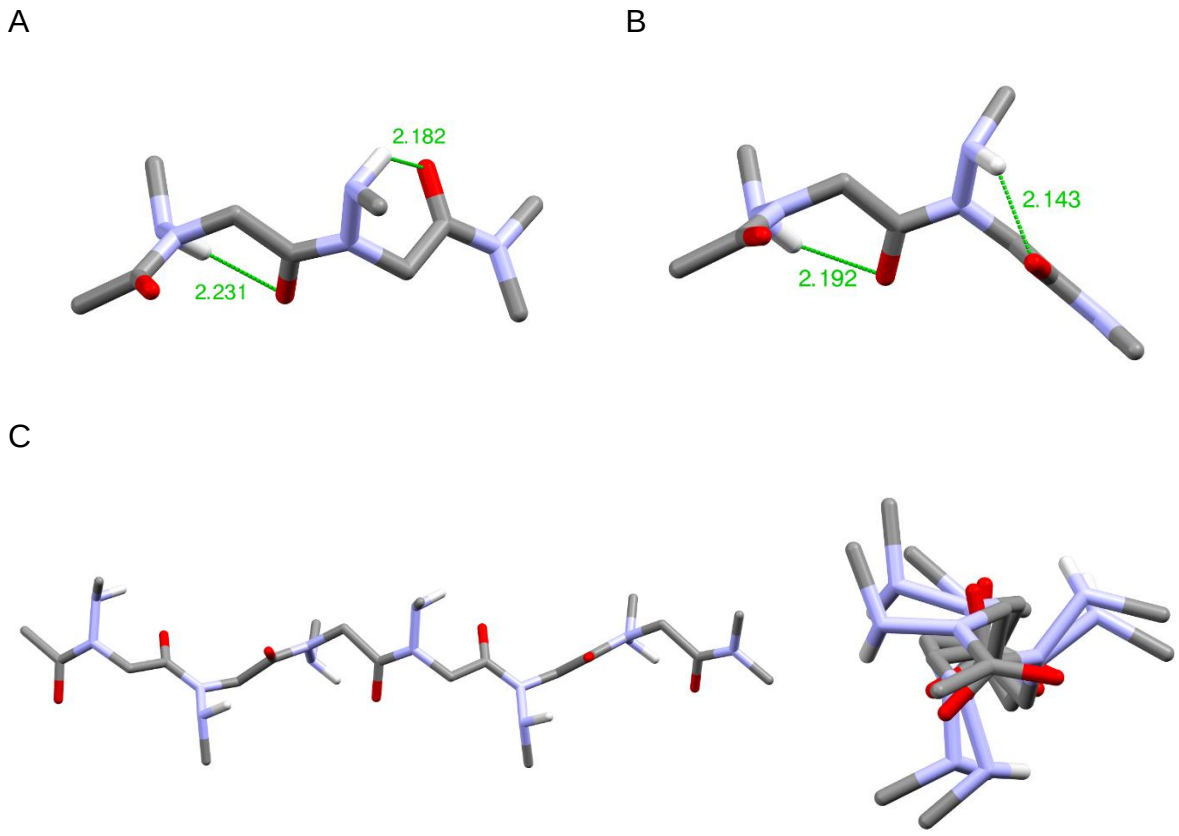

Figure 5. Model structure of *N*-(NMe)glycine peptoid. (A) dimer in the repeating (pp) conformation; (B) dimer in the alternating (pm) conformation; (C) hexamer in the repeating $(p)_6$ conformation: side view (left), perpendicular to helix axis (right).

Conclusion

This report describes for the first time the synthesis of peptoid oligomers consisting of consecutive *N*-alkylamino units, with the aim of creating peptoid oligomers with *trans*-amide linkages. For this first study, we focused on solution-phase synthesis of *N*-methylamino peptoids using a submonomer protocol and evaluated few segment-based coupling methods. The optimisations made with respect to the standard submonomer synthetic conditions will be useful for developing solid-phase synthesis

and access longer and more diverse *N*-alkylamino peptoid oligomers in the future. NMR analysis of the synthesized oligomers **1-6** in various protic and aprotic solvents and of varying polarity indicates that the *N*-(methylamino)glycine units favour *trans*-amides bonds in proportions up to 90% in DMSO-d_6. Adoption of *trans*-amide bonds was confirmed in the crystal structure of dimer **2**. In addition to the control of the amide bond geometry by the *N*-methylamino side chain, the presence of a hydrogen bond NH donor group is a key element in controlling the main-chain conformation and side chains orientation. It should be noted that to date, the presence of D-H donor groups on the side chains has been little exploited to control the folding and intermolecular association properties. The NMR study shows that this peptoid family has a strong propensity to form intermolecular assemblies in solution, whatever the nature of the solvent. TEM images of dimer **2** in water also revealed the formation of multilayered assemblies that deserve to be studied now in more detail. The crystal structure of dimer **2** also reveals the presence of intermolecular hydrogen bonding networks that could potentially be found in solution. It is also interesting to note that despite the lack of chirality, the two residues of peptoid **2** adopt the same conformation in the crystal, reminiscent to that found in helical PPII-like structures. Interestingly, peptoids containing N-methylaminoamides are soluble in water and are capable of forming hydrogen bonds, two interesting characteristics for designing peptidomimetic molecules or biomaterials. Additional efforts are now focused on introducing chirality, which will provide a better understanding of their structural properties, including their potential to form PPII-like helices.

Supporting Information.

Supporting Information File 1: Electronic supplementary information (ESI) available: Experimental procedures, HPLC analytical data, NMR spectra and variable

concentration study, infra-red spectra, full X-ray data for **2**, computation data, and additional TEM images for compound **2**.

File Name: ESI_Taillefumier

File Format: PDF

Supporting Information File 2: crystallographic information file (CIF) for **2,** CCDC deposition number 2167472

File Name: MP420

File Format:

Supporting Information File 3: checkCIF for **2**

File Name: checkcif_MP420

File Format: PDF

Acknowledgements

We express our sincere thanks to M. Leremboure and F. Emenegger for mass spectrometry analyses (UCA PARTNER). We also thank H. Billard and J. Colombet, Plateforme CYSTEM – UCA PARTNER (Clermont-Ferrand, FRANCE), for their technical support and expertise for TEM analyses. We are grateful to the Mésocentre Clermont Auvergne University for providing computing resources.

Funding

This work is partially supported by the French Ministry of Higher Education and Research (grant to MP)

References

1. Simon, R. J.; Kania, R. S.; Zuckermann, R. N.; Huebner, V. D.; Jewell, D. A.; Banville, S.; Ng, S.; Wang, L.; Rosenberg, S.; Marlowe, C. K.; Spellmeyer, D. C.; Tan, R.; Frankel, A. D.; Santi, D. V.; Cohen, F. E.; Bartlett, P. A. *Proc. Natl. Acad. Sci. U. S. A.* **1992**, *89* (20), 9367–9371
2. Zuckermann, R. N. *Biopolymers* **2011**, *96*, 545–555
3. Zuckermann, R. N.; Kodadek, T. *Curr. Opin. Mol. Ther.* **2009**, *11* (3), 299–307
4. Horne, W. S. *Expert Opin. Drug Discov.* **2011**, *6* (12), 1247–1262
5. Lau, K. H. A. *Biomater. Sci.* **2014**, *2* (5), 627–633
6. Kwon, Y. U.; Kodadek, T. *J. Am. Chem. Soc.* **2007**, *129* (6), 1508–1509
7. Miller, S. M.; Simon, R. J.; Ng, S.; Zuckermann, R. N.; Kerr, J. M.; Moos, W. H. *Bioorganic Med. Chem. Lett.* **1994**, *4* (22), 2657–2662
8. Miller, S. M.; Simon, R. J.; Ng, S.; Zuckermann, R. N.; Kerr, J. M.; Moos, W. H. *Drug Dev. Res.* **1995**, *35* (1), 20–32
9. Zuckermann, R. N.; Kerr, J. M.; Moosf, W. H.; Kent, S. B. H. *J. Am. Chem. Soc.* **1992**, *114* (26), 10646–10647
10. Culf, A. S.; Ouellette, R. J. *Molecules* **2010**, *15* (8), 5282–5335
11. Alluri, P. G.; Reddy, M. M.; Bachhawat-Sikder, K.; Olivos, H. J.; Kodadek, T. *J. Am. Chem. Soc.* **2003**, *125* (46), 13995–14004
12. Kwon, Y. U.; Kodadek, T. *Chem. Commun.* **2008**, *0* (44), 5704–5706
13. Gao, Y.; Kodadek, T. *Chem. Biol.* **2013**, *20* (3), 360–369
14. Chiang, Y. C.; Lin, Y. J.; Horng, J. C. *Protein Sci.* **2009**, *18* (9), 1967–1977
15. Vitagliano, L.; Berisio, R.; Mastrangelo, A.; Mazzarella, L.; Zagari, A. *Protein Sci.* **2001**, *10* (12), 2627–2632
16. Sui, Q.; Borchardt, D.; Rabenstein, D. L. **2007**, No. 17, 12042–12048

17. Gorske, B. C.; Stringer, J. R.; Bastian, B. L.; Fowler, S. A.; Blackwell, H. E. *J. Am. Chem. Soc.* **2009**, *131* (45), 16555–16567

18. Kalita, D.; Sahariah, B.; Pravo Mookerjee, S.; Kanta Sarma, B. *Chem. Asian J.* **2022**, Epub ahead of print. PMID: 35362652.

19. Kirshenbaum, K.; Barron, A. E.; Goldsmith, R. A.; Armand, P.; Bradley, E. K.; Truong, K. T. V.; Dill, K. A.; Cohen, F. E.; Zuckermann, R. N. *Proc. Natl. Acad. Sci. U. S. A.* **1998**, *95* (8), 4303–4308

20. Wu, C. W.; Kirshenbaum, K.; Sanborn, T. J.; Patch, J. A.; Huang, K.; Dill, K. A.; Zuckermann, R. N.; Barron, A. E. *J. Am. Chem. Soc.* **2003**, *125* (44), 13525–13530

21. Gorske, B. C.; Bastian, B. L.; Geske, G. D.; Blackwell, H. E. *J. Am. Chem. Soc.* **2007**, *129* (29), 8928–8929

22. Stringer, J. R.; Crapster, J. A.; Guzei, I. A.; Blackwell, H. E. *J. Am. Chem. Soc.* **2011**, *133* (39), 15559–15567

23. Fuller, A. A.; Yurash, B. A.; Schaumann, E. N.; Seidl, F. J. *Org. Lett.* **2013**, *15* (19), 5118–5121

24. Wellhöfer, I.; Frydenvang, K.; Kotesova, S.; Christiansen, A. M.; Laursen, J. S.; Olsen, C. A. *J. Org. Chem.* **2019**, *84* (7), 3762–3779

25. Caumes, C.; Roy, O.; Faure, S.; Taillefumier, C. *J. Am. Chem. Soc.* **2012**, *134* (23), 9553–9556

26. Aliouat, H.; Caumes, C.; Roy, O.; Zouikri, M.; Taillefumier, C.; Faure, S. *J. Org. Chem.* **2017**, *82* (5), 2386–2398

27. Shyam, R.; Charbonnel, N.; Job, A.; Blavignac, C.; Forestier, C.; Taillefumier, C.; Faure, S. *ChemMedChem* **2018**, *13* (15), 1513–1516

28. Wijaya, A. W.; Nguyen, A. I.; Roe, L. T.; Butterfoss, G. L.; Spencer, R. K.; Li, N. K.; Zuckermann, R. N. *J. Am. Chem. Soc.* **2019**, *141* (49), 19436–19447

29. Shyam, R.; Nauton, L.; Angelici, G.; Roy, O.; Taillefumier, C.; Faure, S. *Biopolymers* **2019**, *110* (6), e23273

30. Gimenez, D.; Aguilar, J. A.; Bromley, E. H. C.; Cobb, S. L. *Angew. Chemie Int. Ed.* **2018**, *57* (33), 10549–10553

31. Shin, H. M.; Kang, C. M.; Yoon, M. H.; Seo, J. *Chem. Commun.* **2014**, *50* (34), 4465–4468

32. Rzeigui, M.; Traikia, M.; Jouffret, L.; Kriznik, A.; Khiari, J.; Roy, O.; Taillefumier, C. *J. Org. Chem.* **2020**, *85* (4), 2190–2201

33. Shah, N. H.; Butterfoss, G. L.; Nguyen, K.; Yoo, B.; Bonneau, R.; Rabenstein, D. L.; Kirshenbaum, K. *J. Am. Chem. Soc.* **2008**, *130* (49), 16622–16632

34. Stringer, J. R.; Aaron Crapster, J.; Guzei, I. A.; Blackwell, H. E. *J. Org. Chem* **2010**, *75* (18), 6068–6078

35. Paul, B.; Butterfoss, G. L.; Boswell, M. G.; Renfrew, P. D.; Yeung, F. G.; Shah, N. H.; Wolf, C.; Bonneau, R.; Kirshenbaum, K. *J. Am. Chem. Soc.* **2011**, *133* (28), 10910–10919

36. Crapster, J. A.; Stringer, J. R.; Guzei, I. A.; Blackwell, H. E. *Biopolymers* **2011**, *96* (5), 604–616

37. Jordan, P. A.; Paul, B.; Butterfoss, G. L.; Renfrew, P. D.; Bonneau, R.; Kirshenbaum, K. *Biopolymers* **2011**, *96* (5), 617–626

38. Kanta Sarma, B.; Yousufuddin, M.; Kodadek, T. *Chem. Commun.* **2011**, *47* (38), 10590–10592

39. Sarma, B. K.; Kodadek, T. *ACS Comb. Sci.* **2012**, *14* (10), 558–564

40. Davern, C. M.; Lowe, B. D.; Rosfi, A.; Ison, E. A.; Proulx, C. *Chem. Sci.* **2021**, *12* (24), 8401–8410

41. Huang, N.; Kolhatkar, R.; Eyobo, Y.; Sorci, L.; Rodionova, I.; Osterman, A. L.; MacKerell, A. D.; Zhang, H. *J. Med. Chem.* **2010**, *53* (14), 5229–5239

42. Konig, W.; Geiger, R.; Ber ; Le Nguyen, D.; Castro, B.; Knorr, R.; Trzeciak, A.; Bannworth, W.; Gillessen, D. *Proc. Jpn. Symp. Pept. Chem* **1993**, *115* (2), 36

43. Kang, C. W.; Ranatunga, S.; Sarnowski, M. P.; Del Valle, J. R. *Org. Lett.* **2014**, *16* (20), 5434–5437

44. Liu, F.; Stephen, A. G.; Adamson, C. S.; Gousset, K.; Aman, M. J.; Freed, E. O.; Fisher, R. J.; Burke, T. R. *Org. Lett.* **2006**, *8* (22), 5165–5168

45. Morimoto, J.; Fukuda, Y.; Kuroda, D.; Watanabe, T.; Yoshida, F.; Asada, M.; Nakamura, T.; Senoo, A.; Nagatoishi, S.; Tsumoto, K.; Sando, S. *J. Am. Chem. Soc.* **2019**, *141* (37), 14612–14623

46. Bald, E.; Saigo, K.; Mukaiyama, T. *Chem. Lett.* **1975**, 1163–1166

47. Castelletto, V.; Chippindale, A. M.; Hamley, I. W.; Barnett, S.; Hasan, A.; Lau, K. H. A. *Chem. Commun.* **2019**, *55* (42), 5867–5869

48. Nam, K. T.; Shelby, S. A.; Choi, P. H.; Marciel, A. B.; Chen, R.; Tan, L.; Chu, T. K.; Mesch, R. A.; Lee, B. C.; Connolly, M. D.; Kisielowski, C.; Zuckermann, R. N. *Nat. Mater.* **2010**, *9* (5), 454–460